

Superfluidity in a Doped Helium Droplet

E. W. Draeger[†] and D. M. Ceperley

Department of Physics and National Center for Supercomputing Applications, University of Illinois Urbana-Champaign, 61801

Path Integral Monte Carlo calculations of the superfluid density throughout ^4He droplets doped with linear impurities $(\text{HCN})_n$ are presented. After deriving a local estimator for the superfluid density distribution, we find a decreased superfluid response in the first solvation layer. This effective normal fluid exhibits temperature dependence similar to that of a two-dimensional helium system.

Molecules confined in helium nanodroplets have been shown to exhibit excitation spectra with clearly resolved rotational fine structure consistent with that of a free rotor, though with an increased moment of inertia. Grebenev *et al.* [1] have shown that only a few layers of ^4He coating the molecule are required to decouple the impurity from the droplet and achieve free rotation. Callegari *et al.* [2] have suggested that the increased moment of inertia is due to the hydrodynamic response of the impurity rotating through the anisotropic helium density immediately surrounding the molecule. Kwon and Whalley [3] have proposed a model in which a microscopic normal fluid is induced in the first solvation layer by the anisotropy of the molecule-helium interaction.

In this paper, a microscopic Path Integral Monte Carlo (PIMC) estimator of the local contribution to the total superfluid response is presented. Simulations of ^4He droplets containing linear $(\text{HCN})_3$ isomers show a significant reduction in the superfluid response of the first solvation layer. Furthermore, we find that this reduction is due in part to thermal excitations, in addition to the temperature-independent normal fluid assumed to be induced by the anisotropic HCN-helium interaction potential. The cylindrically-symmetric region of the first solvation layer was found to exhibit temperature dependence consistent with that of a two-dimensional helium system. The moment of inertia was calculated, in reasonable agreement with experiment, and was independent of temperature below $T=1$ K as the dominant contribution came from the normal fluid coating the ends of the molecule, which was predominantly induced by the anisotropy of the density in that region.

The superfluid density can be defined in terms of the response of the system to an imposed rotation. In imaginary-time path integrals, it is manifested by particle exchange over length scales equal to the system size. Although superfluid response (like conductivity) is not itself a local property, it is possible to calculate a local contribution to the total response. In PIMC, the total superfluid response along the axis of rotation \hat{n} is proportional to the square of total projected area of the imaginary-time paths [4]:

$$\frac{\rho_s}{\rho} \Big|_{\hat{n}} = \frac{2m \langle A_{\hat{n}}^2 \rangle}{\beta \lambda I_c}, \quad (1)$$

where $\lambda = \hbar^2/2m$, $\beta = 1/k_B T$ and I_c is the classical

moment of inertia. To define a local superfluid density we write:

$$\begin{aligned} \rho_s(\mathbf{r})|_{\hat{n}} &= \frac{2mN}{\beta \lambda I_c} \left\langle \int d\mathbf{r}' A_{\hat{n}}(\mathbf{r}) A_{\hat{n}}(\mathbf{r}') \right\rangle \\ &= \frac{2mN}{\beta \lambda I_c} \langle A_{\hat{n}}(\mathbf{r}) A_{\hat{n}} \rangle, \end{aligned} \quad (2)$$

where $\mathbf{A}(\mathbf{r})$, related to the local angular momentum operator, is defined as

$$\mathbf{A}(\mathbf{r}) \equiv \frac{1}{2} \sum_{i,k} (\mathbf{r}_{i,k} \times \mathbf{r}_{i,k+1}) \delta(\mathbf{r} - \mathbf{r}_{i,k}) \quad (3)$$

and $A_{\hat{n}}$ is the \hat{n} -component of the total area of all the particles. Since $\mathbf{A}(\mathbf{r})$ integrates to the total area, the local superfluid response exactly integrates to the total response.

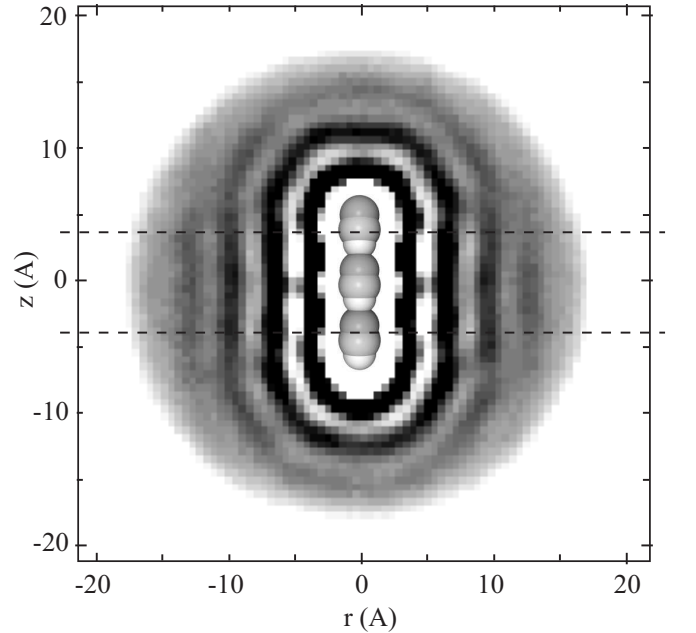


FIG. 1. Average number density of an $N = 500$ $^4\text{He}-(\text{HCN})_3$ droplet at $T = 0.38$ K. The grey scale saturates at $\rho = 0.03 \text{ \AA}^{-3}$ (black). The dashed lines define the cylindrically-symmetric region used for averaging superfluid density.

Two types of contributions to the local superfluid density can be distinguished based on the connectivity of the instantaneous paths: contributions of particles on

the same chain, which on the average must be positive, and contributions of particles on different exchange cycles. By reversing the order of one exchange cycle the contribution from different cycles will change sign; if the cycles are spatially separated, the magnitude of the contribution will be unaffected, so that their contribution is much smaller. They will however increase the statistical noise of the superfluid density. Numerically we find that the same cycle contribution accounts for roughly 80% of the total superfluid density in the systems presented in this paper.

The local superfluid density estimator used by Kwon and Whaley [3] defined the effective normal fluid induced by the anisotropic molecule-helium interaction potential in terms of the average number density distribution of paths in exchange cycles of fewer than six atoms. Although qualitatively interesting, this estimator is not the superfluid response to an imposed rotation, as there is no direct relation between the number of atoms in a permutation cycle and its area.

In order to test our estimator, PIMC simulations were performed on $N = 128$ and $N = 500$ ^4He droplets doped with $(\text{HCN})_3$ isomers. Nauta and Miller [12] found that HCN molecules in helium droplets self-assemble into linear chains spaced roughly 4.4 \AA apart. The HCN molecules in our simulations were fixed along the z -axis with this spacing. An imaginary time-step of $1/20 \text{ K}^{-1}$ was used. With cylindrical symmetry and precise experimental data over a range of isomer lengths, this system is well-suited for studying superfluidity at a molecular interface.

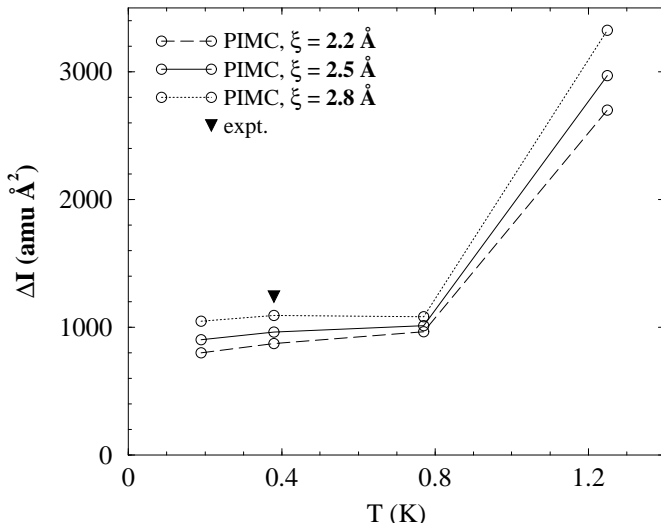


FIG. 2. Temperature dependence of moment of inertia difference of $(\text{HCN})_3$ isomer from the gas phase value due to the helium droplet. Values were calculated from Eq. (4), using the local superfluid density distributions calculated from $N = 128$ PIMC simulations. Also shown is the experimental value for $(\text{HCN})_3$.

The number density of a doped helium droplet at $T = 0.38 \text{ K}$ is shown in Fig. 1. The two-dimensional areal density of the first solvation layer was 0.12 \AA^{-2} , which is still in the liquid phase for thin ^4He films at these temperatures [5]. Even if the density were large enough to be solid in a 2D film, the curved geometry of the film around the HCN molecule could frustrate crystalline order, keeping the first solvation layer in a dense liquid state.

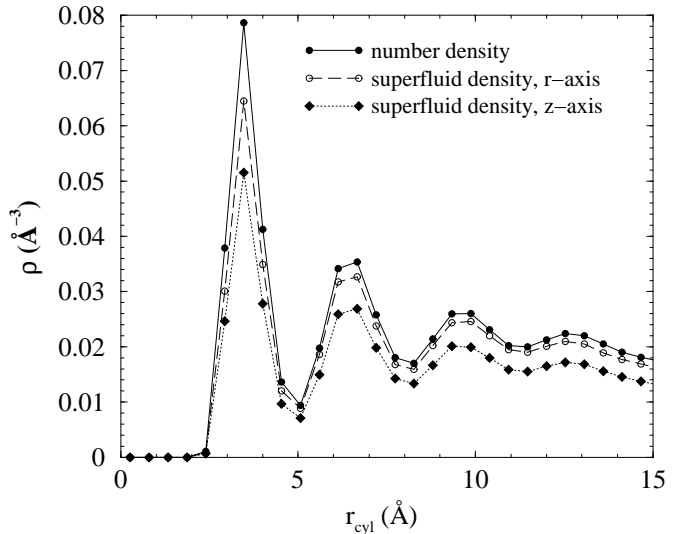


FIG. 3. Superfluid and number density distributions, averaged over the cylindrically-symmetric region of an $N = 500$ ^4He - $(\text{HCN})_3$ droplet at $T = 0.38 \text{ K}$.

We define the change in the moment of inertia due to the helium as the contribution due to the normal fraction in the first layer rotating rigidly with the impurity:

$$\Delta I = \int_{v(\xi)} d\mathbf{r} m_4 r_{\perp}^2 (\rho(\mathbf{r}) - \rho_s(\mathbf{r})) \quad (4)$$

where $v(\xi)$ is the volume of helium a distance ξ away from the surface of the molecule, r_{\perp} is the radial distance from the axis of rotation in cylindrical coordinates. The results calculated from our $N = 128$ droplet results are plotted in Fig. 2, for several cutoff distances near the first layer minimum. Both the estimated statistical error and the uncertainty due to the cut-off were on the order of 10%. Fig. 2 shows that the moment of inertia due to the effective normal fluid in the first solvation layer calculated using our PIMC local superfluid density estimator is in reasonable agreement with the experimental value of $\Delta I = 1240 \text{ amu \AA}^2$ [11], within error bars. We also find that ΔI is effectively independent of temperature below $T = 1.0 \text{ K}$. This is because the dominant contribution to the moment of inertia comes from the induced normal fluid at the ends of the isomer, which is almost completely due to anisotropy in the molecular potential.

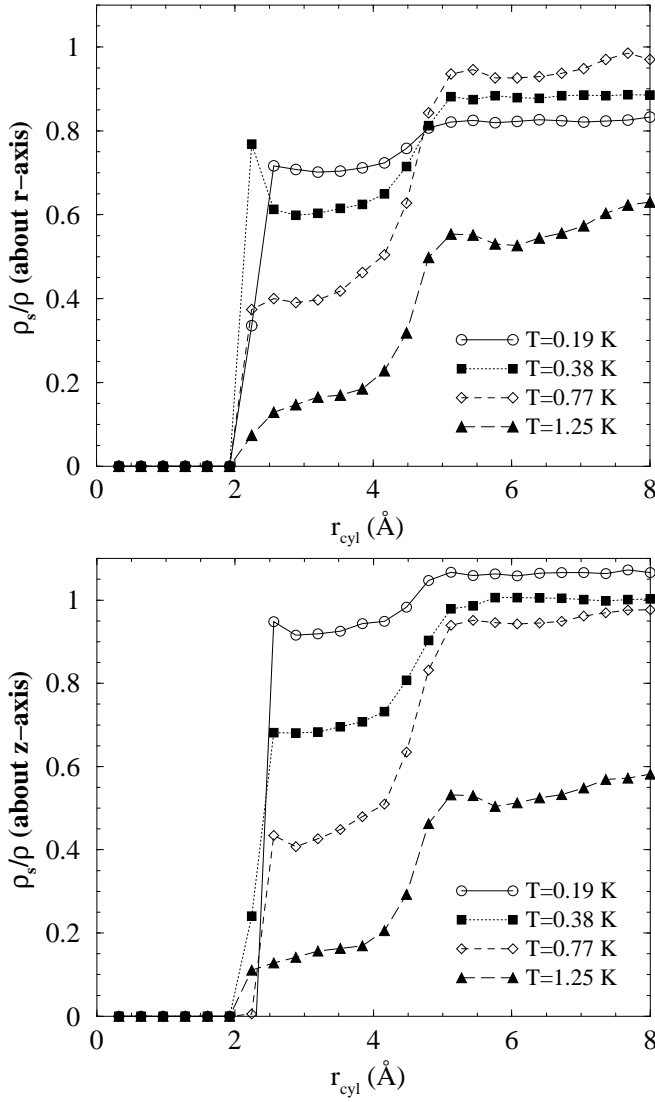


FIG. 4. Superfluid density fraction distributions, averaged over the cylindrically-symmetric region of an $N = 128$ $^4\text{He}(\text{HCN})_3$ droplet at $T = 0.19, 0.38, 0.77$, and 1.25 K. The top graph shows superfluid response about the radial axis, the bottom graph shows superfluid response about the molecule axis.

To quantify the reduced superfluid response in the first layer, we averaged over the cylindrically-symmetric region of the $^4\text{He}(\text{HCN})_3$ droplet, defined as the region between $z = -3.5$ Å and $z = 3.5$ Å (see Fig. 1). The results of this averaging are shown in Fig. 3. Taking the ratio of the superfluid density to the number density clearly shows a reduced superfluid response in the first layer for rotation about both the radial axis and the molecular axis. At zero temperature, there can be no “normal” density for rotation about the molecular axis because of the cylindrical symmetry, so this reduction must be due to thermal excitations.

Shown in Fig. 4 is the temperature dependence of the

superfluid density in the first solvation layer, determined for $N = 128$ $^4\text{He}(\text{HCN})_3$ droplets at $T = 0.19, 0.38, 0.77$, and 1.25 K. At first glance, this result appears to contradict known properties of liquid helium; the superfluid density of bulk helium at 0.75 K is $1.000(1)$. Theoretical studies of pure $N = 128$ helium clusters show a superfluid transition roughly in agreement with the bulk lambda transition [6]. Pure droplets like those produced for use in scattering experiments, with several thousand atoms at $T = 0.38$ K, should have a superfluid fraction very close to unity. However, the helium in the first layer coating the impurity molecule more closely resembles a two-dimensional system than a three-dimensional system, because the motion of the helium atoms is restricted by the He-HCN potential to be primarily on the cylindrical surface circumscribing the $(\text{HCN})_3$ impurity. Two-dimensional helium films have been shown to have a Kosterlitz-Thouless type of superfluid transition at temperatures significantly lower than T_λ [7,8]. The reduction in the transition temperature is due to the reduced dimensionality, increasing the phase space for long wavelength fluctuations, and the lowering of the “roton” gap. A similar temperature-dependent reduction in the superfluid response of the first layer of helium surrounding the ends of the isomer was not observed.

To extract the average superfluid density fraction in the first layer from the distributions plotted in Fig. 4, we integrate over the superfluid density and number density in the first layer and take the ratio:

$$\frac{\rho_s}{\rho} = \frac{\int_0^{r_1} dr_{cyl} \rho_s(r_{cyl})}{\int_0^{r_1} dr_{cyl} \rho(r_{cyl})}, \quad (5)$$

where r_1 is the position of the density minimum between the first and second solvation layers. The average superfluid density in the first solvation layer as a function of temperature is shown in Fig. 6. The transition is very broad due to the small number of atoms (~ 30) in the first layer. It shows the onset of superfluidity at roughly 1 K. The superfluid density about the molecule axis (z-axis) goes to unity as the temperature goes to zero, as the density is symmetric about this axis. The normal fluid response from rotating about the radial axis (r-axis) combines both thermal effects and effective normal fluid induced by rotating through the anisotropic helium density, and because of this, does not go to zero at $T = 0$ K [2].

We have determined that only a small fraction of the particles in the first layer are localized (not permuting) at $T=0.38$ K and below, as shown in Fig. 5. Though many of the permutations are between atoms within the same layer, the first layer is not cut off from the rest of the fluid. Below 1 K, the majority of the atoms in the droplet are part of exchange cycles with atoms in both

the first layer and the rest of the droplet. However, in terms of excitations, the first layer is well represented as a 2D superfluid.

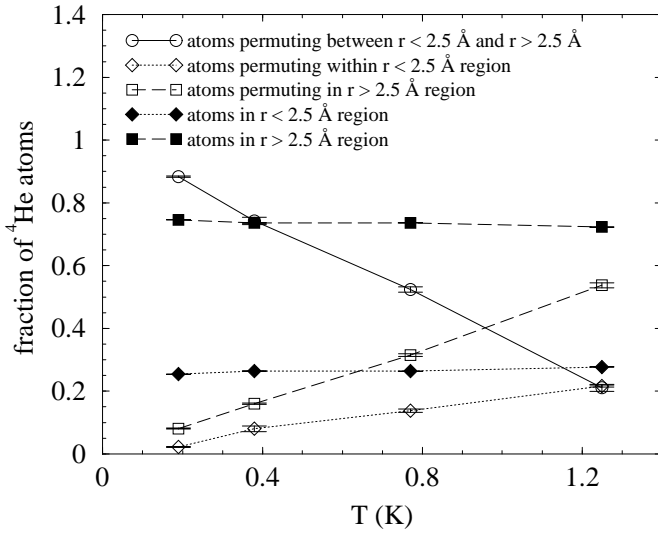


FIG. 5. Exchange behavior of the first layer (defined as 2.5 Å or less from the surface of the $(\text{HCN})_3$ isomer) as a function of temperature. A permutation cycle was considered to be part of the first layer if more than $M/2$ consecutive time slices were contained within it, where M is the number of imaginary time slices per atom.

To compare the effects of density on the thermally-induced normal fluid in the first layer, we calculated the superfluid density distribution for $N = 128$ $^4\text{He}-(\text{HCN})_3$ droplets at $T=0.19, 0.38, 0.77$, and 1.25 K, with a ^4He -HCN interaction reduced by a factor of two in order to reduce the density in the first solvation layer. The density in the first layer decreased by $\sim 15\%$, corresponding to an average coverage of 0.10 \AA^{-2} . The difference in coverage caused a 20% reduction in the superfluid response about the radial axis at $T=0.19$ K and $T=0.38$ K. At higher temperatures, the superfluid response was unchanged within the estimated error bars. The superfluid response about the molecule axis (z-axis) was unchanged within error bars. This is further evidence that the normal response in the first layer is due to both the anisotropy of the molecular potential and thermal excitations.

Using PIMC and a local superfluid density estimator, we find that the first solvation layer surrounding a linear impurity is approximately a two-dimensional superfluid. Although this effect has only a small contribution to the moment of inertia of this system, it is clear that thermal excitations play a significant role in the superfluid surrounding a molecule. By varying the temperature of the droplet, by adding ^3He atoms, one could, in principle, observe such temperature dependence in the moment of inertia.

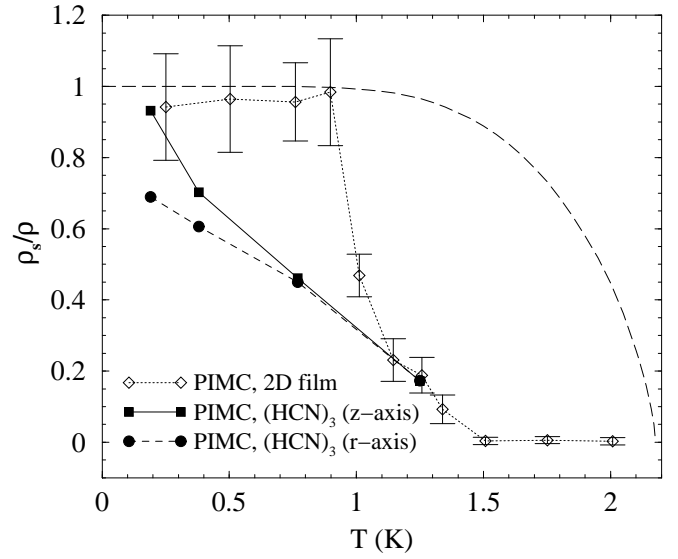


FIG. 6. Superfluid density fraction of the cylindrically-symmetric portion of the first layer of an $N = 128$ $^4\text{He}-(\text{HCN})_3$ droplet vs. temperature, calculated using Eq. (5). The first layer in these systems has an estimated coverage of $\sigma = 0.12 \text{ \AA}^{-2}$. Superfluid response about both the molecule axis (solid squares) and radial axis (solid circles) are presented. Also shown are the PIMC results of Gordillo et al (open diamonds), for a 2D ^4He film with $\sigma = 0.051 \text{ \AA}^{-2}$. For reference, the superfluid transition in bulk ^4He is included (dashed line).

The authors would like to acknowledge K. Lehmann and B. Whaley for useful discussions. The computations were carried out at NCSA and the IBM cluster at the Materials Computation Center, and was supported by the NASA Microgravity Research Division, Fundamental Physics Program. This work was also performed under the auspices of the U.S. Department of Energy by University of California Lawrence Livermore National Laboratory under contract No. W-7405-Eng-48.

† Present Address: Lawrence Livermore National Laboratory, 7000 East Avenue, L-415, Livermore, CA 94550.

-
- [1] Grebenov, S., J. P. Toennies and A. F. Vilesov, *Science* **279**, 2083 (1998).
 - [2] Callegari, C., A. Conjusteau, I. Reinhard, K. K. Lehmann, G. Scoles and F. Dalfvo, *Phys. Rev. Lett.* **83**, 5058 (1999).
 - [3] Kwon, Y. and K. B. Whaley, *Phys. Rev. Lett.* **83**, 4108 (1999).
 - [4] Pollock, E. L. and D. M. Ceperley, *Phys. Rev. B* **36**, 8343 (1987).
 - [5] Bishop, D. J., J. E. Berthold, J. M. Parpia and J. D.

- Reppy, Phys. Rev. B **24**, 5047 (1981).
- [6] Sindzingre, P., M. L. Klein and D. M. Ceperley, Phys. Rev. Lett. **63**, 1601 (1989).
 - [7] Ceperley, D. M., and Pollock, E. L., Phys. Rev. B **39**, 2084 (1989)
 - [8] Nyéki, J., R. Ray, V. Maidanov, M. Siqueira, B. Cowan and J. Saunders, J. Low Temp. Phys. **101**, 279 (1995).
 - [9] Gordillo, M. C. and D. M. Ceperley, Phys. Rev. B **58**, 6447 (1998).
 - [10] Kim, K. and W. F. Saam, Phys. Rev. B **48**, 13735 (1993).
 - [11] Nauta, K., private communication (2001).
 - [12] Nauta, K. and R. E. Miller, Science **283**, 1895 (1999).
 - [13] Goyal, S., D. L. Schutt and G. Scoles, Phys. Rev. Lett. **69**, 933 (1992).
 - [14] Pi, M., R. Mayol and M. Barranco, Phys. Rev. Lett. **82**, 3093 (1999).
 - [15] Ceperley, D. M., Rev. Mod. Phys. **67**, 279 (1995).
 - [16] Lehmann, K. K., Mol. Phys. **97**, 645 (1998).
 - [17] Toennies, J. P. and A. F. Vilesov, Annu. Rev. Phys. Chem. **49**, 1 (1998).
 - [18] Atkins, K. M. and J. M. Hutson, J. Chem. Phys. **105**, 440 (1996).
 - [19] Kwon, Y., P. Huang, M. V. Patel, D. Blume and K. B. Whaley, J. Chem. Phys. **113**, 6469 (2000).